

# Maximal Success Probabilities of Linear-Optical Quantum Gates

Dmitry B. Uskov<sup>1</sup>, Lev Kaplan<sup>1</sup>, A. Matthew Smith<sup>1</sup>, Sean D. Huver<sup>2</sup>, and Jonathan P. Dowling<sup>2</sup>

<sup>1</sup>*Department of Physics, Tulane University, New Orleans, Louisiana 70118*

<sup>2</sup>*Hearne Institute for Theoretical Physics, Department of Physics and Astronomy, Louisiana State University, Baton Rouge, Louisiana 70803*

(Dated: April 14, 2022)

Numerical optimization can be used to design linear-optical devices that produce a desired quantum state, or implement a desired quantum gate with perfect fidelity, while maximizing the success probability. In the case of the two-qubit CS (or CNOT) gate, we provide numerical evidence that the maximum success rate is  $2/27$ , when two unentangled ancilla resources are available. Interestingly, in light of a much larger upper bound obtained analytically [1], we find that additional unentangled ancillas do not increase the success probability. As an example of a three-qubit logic gate, we consider the Toffoli gate and show that obtaining perfect fidelity requires a minimum of four unentangled ancillas. Using a restricted search subspace inspired by Knill [2], we obtain a maximum success rate of 0.00340. This result compares well with the success rate of  $(2/27)^2/2 \approx 0.00274$ , which can be obtained using the same resources by combining two CNOT gates and a passive quantum filter [3]. The general optimization approach could easily be applied to other areas of interest, such as quantum imaging, quantum error correction, and cryptography [4, 5, 6].

PACS numbers: 03.67.-a, 03.67.Lx, 42.50.Dv

Linear optics is considered as a viable method for scalable quantum information processing, due in large part to the seminal work of Knill, Laflamme, and Milburn (KLM) [7]. These authors showed that an elementary quantum logic gate on qubits, encoded in photonic states, can be constructed using a combination of linear-optical elements and quantum measurement. The trade-off in this measurement-assisted scheme is that the gate is properly implemented only when the measurement yields a positive outcome, i.e., the gate has non-deterministic character. Soon after the KLM scheme became a paradigm for the linear quantum computation (LOQC) it became clear that there is serious unresolved theoretical problem of how to find the optimal implementation of desired quantum transformation (inverse linear optical state generator (LOQCG) problem [9]). The problem has the same character of complexity as the problem of modeling quantum computers using classical computers, and a major task of theoretical research on the inverse LOQCG problem is to find analytical or numerical way to design linear-optics devices that implement single gates, as well as combinations of gates, with the highest possible success probabilities, while maintaining perfect or near-perfect gate fidelity.

For the nonlinear sign (NS) gate, which acts on photons in a single optical mode,  $\alpha_0|0\rangle + \alpha_1|1\rangle + \alpha_2|2\rangle \rightarrow \alpha_0|0\rangle + \alpha_1|1\rangle - \alpha_2|2\rangle$ , the maximum success probability without feed-forward has been theoretically proved to be  $1/4$  [8]. Here we focus on more complicated gates, taking as examples the two-qubit controlled sign (CS) gate (equivalently, the CNOT gate), and the three-qubit Toffoli gate. For these physically important gates, existing theoretical results are limited to upper or lower bounds on the success probability [1, 2, 3].

A linear-optical quantum gate, or state generator (LO-

QSG) [9], can be viewed formally as a device implementing a contraction transformation (for ideal detectors) that converts pure input states into desired pure output states. The goal of the optimization problem is to find a proper linear optical network (see Fig. 1), characterized by a unitary matrix  $U$ , that performs the desired transformation [10, 11]. The problem is naturally partitioned into two tasks - i) finding a subspace of perfect fidelity and ii) maximizing the success probability within this subspace. While in this paper we address transformations implemented by linear optics, the method is universal and with minor modifications can be efficiently applied to any quantum-information problem involving unitary operations combined with measurements.

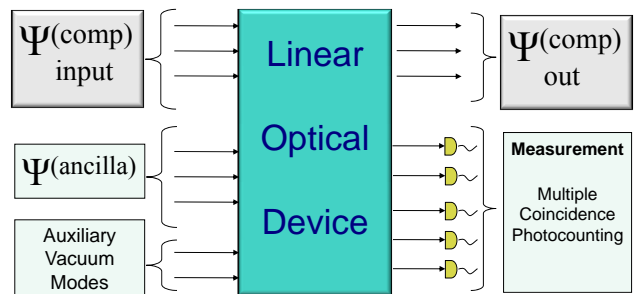


FIG. 1: A general measurement-assisted transformation (e.g., a quantum logic gate or a linear-optical quantum state generator). It exploits linear operations, followed by a set of measurements in auxiliary modes to convert an input state into a target output state.

Historically, the linear-optical device was envisioned as a network of linear-optical elements [12], as for example in the original KLM scheme, where the CS gate is constructed as a combination of two NS gates [7]. In prac-

tice, building a functional microchip-based device does not require partitioning the transformation into blocks. Instead, the whole device may be considered as an integrated light circuit [12], performing one large operation, as shown schematically in Fig. 1. Here the input state  $|\Psi_{\text{in}}\rangle = |\Psi_{\text{in}}^{\text{comp}}\rangle \otimes |\Psi_{\text{in}}^{\text{ancilla}}\rangle \otimes |\Psi^{\text{vacuum}}\rangle$  is a product of a computational input state, an ancilla state, and possibly a vacuum state. Assuming dual-rail encoding, the computational state will consist of  $M_c$  photons in  $N_c = 2M_c$  optical modes encoding an arbitrary state of  $M_c$  qubits, e.g., the logical two-qubit state  $|\uparrow\rangle \otimes |\uparrow\rangle$  may be represented in four optical modes by  $|1_1, 0_2\rangle \otimes |1_3, 0_4\rangle$  in the Fock basis. The ancilla input state of  $M_a$  photons distributed over  $N_a$  modes may be a separable state, an entangled state, or even half of an ebit state carrying spatially distributed entanglement, as required for example in entanglement-assisted error correction [4, 13]. Finally,  $N_v$  auxiliary vacuum modes contain zero photons in the initial state.

The core of the device is the transformation  $a_i^{(in)\dagger} \rightarrow U_{i,j} a_j^{(out)\dagger}$  of the photon creation operators between the input and output states. Here  $U$ , which contains all physical properties of the device, is an  $N \times N$  unitary matrix, where  $N = N_c + N_a + N_v$  is the total number of modes. The matrix  $U$  associated with the physical device induces a transformation  $\hat{\Omega}$  acting on the input state, where  $\hat{\Omega}$  is a high-dimensional irreducible representation of  $U$  [14]. Writing the total input state in the Fock representation as  $|\Psi_{\text{in}}\rangle = |n_1, n_2, \dots, n_N\rangle$ , where  $\sum n_i = M_c + M_a$  is the total number of photons,  $\hat{\Omega}$  takes the form

$$|\Psi_{\text{out}}\rangle = \hat{\Omega}|\Psi_{\text{in}}\rangle = \prod_{i=1}^N \frac{1}{\sqrt{n_i!}} \left( \sum_{j=1}^N U_{i,j} a_j^{(out)\dagger} \right)^{n_i} |0\rangle. \quad (1)$$

Next, a measurement is applied to the  $N_c$  ancilla and vacuum modes. This measurement is formally described by a Kraus POVM operator acting on these modes only:  $\hat{P} = |0_{N_c+1}, 0_{N_c+2}, \dots, 0_N\rangle \langle \Psi_{\text{measured}}|$ . In the most natural case of a photocounting measurement,  $\langle \Psi_{\text{measured}}| = \langle k_{N_c+1}, k_{N_c+2}, \dots, k_N|$ , where  $k_i$  is the number of photons measured in the  $i$ -th mode. Finally, the resulting transformation of the computational state is a contraction quantum map  $|\Psi_{\text{out}}^{\text{comp}}\rangle = \hat{A}|\Psi_{\text{in}}^{\text{comp}}\rangle / \|\hat{A}|\Psi_{\text{in}}^{\text{comp}}\rangle\|$  [15], where  $\hat{A}$  is defined by

$$\hat{A}|\Psi_{\text{in}}^{\text{comp}}\rangle = \langle k_{N_c+1}, k_{N_c+2}, \dots, k_N | \hat{U} | \Psi_{\text{in}} \rangle. \quad (2)$$

The linear operator  $\hat{A}$  contains all the information of relevance to the gate or state transformation.

Now we consider the main properties of Eq. (2) relevant to the optimization problem. In the Fock basis, the matrix  $\hat{A}$  is a submatrix of the larger matrix  $\hat{\Omega}$ , and in accordance with Eq. (1), matrix elements of  $\hat{A}$  are given as polynomials of degree  $M_c + M_a$  in the matrix elements

of  $U$ . The largest number of terms in the polynomial occurs when all initial and final occupation numbers are 0 or 1, in which case the matrix element of  $\hat{A}$  is a sum over permutations of the occupied modes, i.e., the polynomial consists of  $(M_c + M_a)!$  terms of degree  $M_c + M_a$ . For example, the matrix element for transforming the two-qubit computational state  $|\uparrow\rangle \otimes |\uparrow\rangle$  into  $|\uparrow\rangle \otimes |\downarrow\rangle$ , with two ancilla photons in modes 5 and 6, is

$$\langle 1_1 0_2 0_3 1_4 | \hat{A} | 1_1 0_2 1_3 0_4 \rangle = \sum_{\substack{j_1, j_2, j_3, j_4 \\ = \text{permutations } (1,3,5,6)}} U_{1,j_1} U_{4,j_2} U_{5,j_3} U_{6,j_4}. \quad (3)$$

More generally, in the Fock representation, all matrix elements are calculated as permanents of  $U$  [9].

Furthermore, if the total number of measured photons  $\sum_{i=N_c+1}^N k_i$  is the same as the number of input ancilla photons  $\sum_{i=N_c+1}^N n_i$ , then Eq. (2) leaves the number of computational photons invariant. The dual-rail computational basis is a subset of all possible states of  $M_c$  photons in the  $2M_c$  computational modes. Thus, the transformation matrix  $\hat{A}$  is a rectangular matrix, mapping the computational Hilbert space, of dimension  $2^{M_c}$ , to a larger Hilbert space, of dimension  $(3M_c - 1)! / (2M_c - 1)! (M_c)!$ . For example,  $\hat{A}$  is a  $10 \times 4$  matrix for a two-qubit gate, a  $56 \times 8$  matrix for a three-qubit gate and  $35 \times 9$  for two-mode biphotonic qutrit gates [16]. Thus, all quantities of interest, such as the success rate and fidelity of a gate, can be expressed in terms of a relatively small number of matrix elements, despite the large dimension of the underlying Hilbert space. We also note that for a LOQSG problem, as opposed to a gate, only one column of  $\hat{A}$  is of interest, corresponding to a specific input state.

We now define precisely the operational fidelity of a transformation, which in general differs from the common measure of fidelity for a state transformation [17]. Physically, the transformation  $\hat{A}$  has 100% fidelity if it is proportional to the target transformation operation  $\hat{A}^{\text{Tar}}$ , i.e.,  $\hat{A} = g \hat{A}^{\text{Tar}}$ , where  $g$  is an arbitrary complex number (in which case  $S = |g|^2$  is the success probability of the transformation [18]). In general, we may consider complex rays  $\beta_1 \hat{A}$  and  $\beta_2 \hat{A}^{\text{Tar}}$ ,  $\beta_1, \beta_2 \in \mathbb{C}$  as elements of a complex projective space, and define the fidelity as

$$F(\hat{A}) = \frac{\langle \hat{A} | \hat{A}^{\text{Tar}} \rangle \langle \hat{A}^{\text{Tar}} | \hat{A} \rangle}{\langle \hat{A} | \hat{A} \rangle \langle \hat{A}^{\text{Tar}} | \hat{A}^{\text{Tar}} \rangle}, \quad (4)$$

where the Hermitian inner product is  $\langle \hat{A} | \hat{B} \rangle \equiv \text{Tr}(\hat{A}^\dagger \hat{B}) / D_c$ , and  $D_c = 2^{M_c}$  is the dimension of the computational space.  $F$  is closely related to the Fubini-Study distance  $\gamma = \cos^{-1}(\sqrt{F})$  [19], but for numerical computations  $F$  has the advantage of being non-singular near  $F = 1$ .

In general, the success probability  $S$  depends on the initial state  $|\Psi_{\text{in}}^{\text{comp}}\rangle$ .  $S$  is bounded above by the operator

norm  $\|\hat{A}\|_{\text{Max}} = \text{Max}(\langle \Psi_{\text{in}}^{\text{comp}} | \hat{A}^\dagger \hat{A} | \Psi_{\text{in}}^{\text{comp}} \rangle)$ , and below by  $\|\hat{A}\|_{\text{Min}} = \text{Min}(\langle \Psi_{\text{in}}^{\text{comp}} | \hat{A}^\dagger \hat{A} | \Psi_{\text{in}}^{\text{comp}} \rangle)$ , where the maximum and minimum are taken over the set of properly normalized input states. As a more convenient measure, we use the Hilbert-Schmidt norm  $\|\hat{A}\|_{\text{(HS)}} = \text{Tr}(\hat{A}^\dagger \hat{A})/D_c$ . It is easy to verify that  $\|\hat{A}\|_{\text{Min}} \leq \|\hat{A}\|_{\text{(HS)}} \leq \|\hat{A}\|_{\text{Max}}$ . As fidelity  $F \rightarrow 1$ ,  $\|\hat{A}\|_{\text{Min}}/\|\hat{A}\|_{\text{Max}} \rightarrow 1$  and  $S$  becomes a well-defined quantity equal to  $\|\hat{A}\|_{\text{(HS)}}^2$ . We refer to  $\|\hat{A}\|_{\text{(HS)}}^2$  as *the success probability*, keeping in mind that it may not correspond to the success probability for every initial state, except in the case of perfect fidelity.

The two-qubit CS gate may be defined as  $|0101\rangle \rightarrow -\alpha|0101\rangle$ , and  $|\Psi_{\text{in}}^{\text{comp}}\rangle \rightarrow \alpha|\Psi_{\text{in}}^{\text{comp}}\rangle$  for  $\langle 0101 | \Psi_{\text{in}}^{\text{comp}} \rangle = 0$  (for a complex constant  $\alpha$ ). Here  $\hat{A}$  is a  $10 \times 4$  matrix, and the success  $S$  has the form

$$S(U) = \frac{1}{4} \sum_{i=1}^{10} \sum_{j=1}^4 |A_{ij}(U)|^2. \quad (5)$$

The corresponding fidelity function is

$$F(U) = \frac{1}{4} \left| \sum_{j=1}^3 A_{jj}(U) - A_{44}(U) \right|^2 / \sum_{ij} |A_{ij}(U)|^2, \quad (6)$$

where  $A_{11}$ ,  $A_{22}$ ,  $A_{33}$ , and  $A_{44}$  are coefficients that transform computational input state  $|1010\rangle$ ,  $|1001\rangle$ ,  $|0110\rangle$ , and  $|0101\rangle$ , respectively, into the same output state. For a different number of ancilla resources, the form of Eqs. (5) and (6) remains identical; only the matrix elements  $A_{ij}(U)$  need to be recomputed in accordance with Eqs. (1), (2) as permanents of the appropriately-sized matrix  $U$ .

Once the success rate  $S(U)$  and fidelity  $F(U)$  have been constructed for a given target transformation and given ancilla resources, the task is to find the unitary matrix  $U$  that maximizes  $S(U)$  on the constraint set  $F(U) = 1$ . Obviously there are many effective ways to approach this numerical problem: the choice we present below has good convergence properties for the several examples we consider here. We parametrize  $U = \exp(\sum_{j=1}^{N^2} x_j H_j)$ , where  $H_j$  is a complete set of complex anti-Hermitian  $N \times N$  matrices, and find a local maximum of  $F$  in  $x$  space. Once the optimization has converged, we check whether  $F = 1$  to numerical accuracy, in which case we proceed to find a local maximum of success probability  $S$  on the  $F = 1$  surface. Repeating the process with multiple randomly chosen starting points, we obtain the best  $S$ , which yields the optimal design for the quantum circuit.

We first apply our approach to the CS gate. Here, one easily checks that the minimum number of unentangled ancillas needed to obtain perfect fidelity is two, so that  $U$  is a  $6 \times 6$  matrix ( $N = N_c + N_a = 4 + 2 = 6$ ). In this case, we find that the second optimization stage is unnecessary, i.e., the success is a constant on every  $F = 1$  manifold (each such manifold consisting of an

equivalence class of matrices differing only by phase factors). Several inequivalent  $F = 1$  manifolds are found. The best solutions have  $S = 2/27$ , corresponding to an analytic solution found previously by Knill [2], and additional solutions obtained from Knill's matrix by phases and discrete symmetries that simultaneously preserve  $F$  and  $S$ . Due to the complexity of the CS gate, it is not known if an analytical proof for determining the maximum success probability is possible. Our numerical evidence, however, strongly indicates that Knill's solution is indeed the global maximum.

Can the solution be improved by adding  $N_v$  vacuum modes to the device? This question may be answered straightforwardly by repeating the above optimization with  $(6 + N_v) \times (6 + N_v)$  unitary matrices  $U$ , for various values of  $N_v$ . However, there exists an alternative "unitary dilation" approach [9]. Note that matrix elements  $\hat{A}_{ij}$  remain permanents of the upper left  $6 \times 6$  submatrix of  $U$ , since the  $N_v$  vacuum modes have zero occupation number in both the initial and final projected states. Now a  $6 \times 6$  submatrix of a  $(6 + N_v) \times (6 + N_v)$  unitary matrix is subunitary, with at most  $N_v$  singular values below unity; conversely any  $6 \times 6$  subunitary matrix with  $N_v$  singular values below unity may always be extended to a  $(6 + N_v) \times (6 + N_v)$  unitary matrix. Thus, adding  $N_v$  vacuum modes is equivalent to relaxing the unitarity condition on the  $6 \times 6$  matrix  $U$ , and allowing up to  $N_v$  singular values to be subunitary. The most general device design, allowing for an arbitrary number of vacuum modes, is obtained by allowing  $U$  to be an arbitrary complex  $6 \times 6$  matrix, and replacing  $U \rightarrow U/\sqrt{\|U\|_{\text{Max}}}$ , which scales the maximum singular value to unity. The expression for fidelity as a function of  $U$  (Eq. (4), or specifically Eq. (6)) is invariant under scaling, while the generalized success function for a nonunitary  $U$  is given by

$$\tilde{S}(U) = S(U)/(\|U\|_{\text{Max}})^{M_c + M_a}. \quad (7)$$

$\tilde{S}(U)$  has a discontinuous gradient whenever the largest singular value of  $U$  goes through a double or higher-order degeneracy. Of particular interest is the fact that  $\tilde{S}$ , while well-behaved on the manifold of unitary matrices  $U$ , has a singular cusp-like structure in the neighborhood of this manifold.

The result of a non-unitary optimization for the CS gate with two ancillas is shown in Fig. 2. Each point may correspond to a local maximum of the success rate. However, using more accurate numerical analysis, we found that in the region of success probability  $s > 0.04$  we can identify only two local maxima,  $s \approx 0.047$  and  $s = 2/27 \approx 0.074$ . The  $s = 2/27 \approx 0.074$  maximum has much larger basin of attraction than the  $s \approx 0.047$  maximum (the  $s \approx 0.0625$  may be also a local maximum with very small basin of attraction). Random sampling of data points from about 1700 points shown on the Fig. 2 for 2 ancillas reveals that if the optimization algorithm is continued for much larger number of iterations with

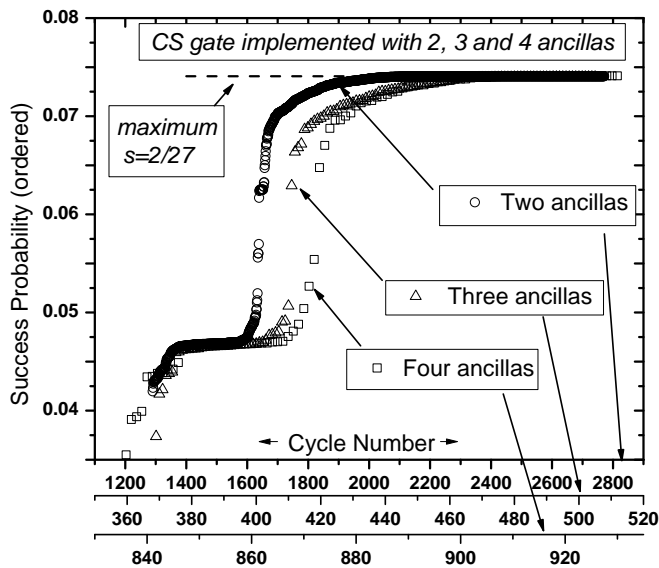


FIG. 2: The optimized success probability for the CS gate is shown for two, three, and four ancillas, and an arbitrary number of vacuum modes. Each point indicates a complete run starting from a randomly chosen starting matrix  $U$ . The success rates are arranged in ascending order, so that the horizontal axis may be viewed as a cumulative probability. The  $2/27 \approx 0.074$  success rate found by Knill [2] is indicated by a horizontal line.

higher numerical accuracy the optimization converges to one of two local maxima. The existence of pronounced plateau at  $2/27$  provides strong numerical evidence that Knill’s solution (which makes no use of vacuum modes) is globally optimal, even when vacuum modes are allowed. It appears that the cusp-like structure of the success rate (7) strongly favors maxima appearing at unitary values of  $U$  (where all singular values become degenerate at 1), and indeed the global maximum corresponds to one such unitary matrix: the Knill matrix. Interestingly, analytical fidelity-preserving transformations, constructed by extending the Gröbner basis method [9], can explain only seven dimensions of the  $F = 1$  subspace, while direct numerical tests reveals that this subspace is 11-dimensional in the vicinity of the Knill solution. This indicates that there exist hidden symmetries, which, we believe, can be identified only by more powerful mathematical methods from the repertoire of algebraic geometry.

Next, we investigate the effect that additional ancilla resources may have on the optimization problem. Previously, an upper bound for the success probability with unentangled resources was shown to be  $3/4$  [1]. Repeating our optimization procedure in larger matrix spaces associated with three and four ancillas, we find, surprisingly, that the global maximum is unchanged. This suggests that the minimum resources needed to produce the CS gate with perfect fidelity (i.e., two unentangled ancillas with no vacuum modes) also suffice to produce the

best possible success rate. In view of the fact that exactly the same behavior of success probability has been found for the NS gate [8] one may expect that this may be a universal property of probabilistic (photonic) gates: *the maximal success probability is attained with minimal required resources.*

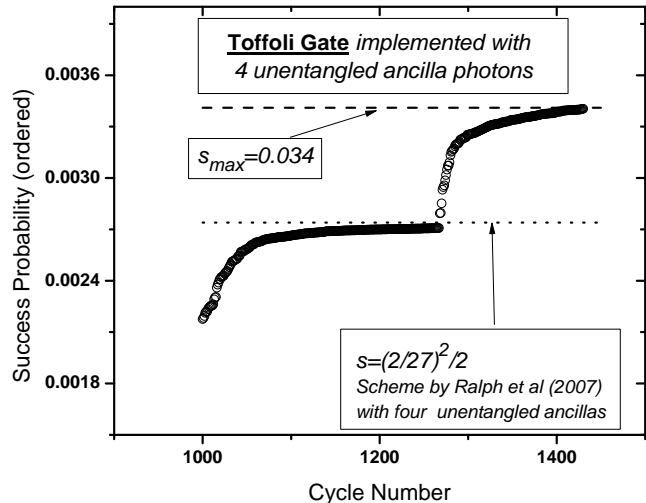


FIG. 3: The distribution of success probabilities for the Toffoli gate.

Next we consider three-qubit (Controlled Sign) Toffoli gate. After a local Hadamard rotation, the standard Toffoli gate acts as a “sign” transformation:  $|010101\rangle \rightarrow \alpha|010101\rangle$ , and  $|\Psi_{\text{in}}^{\text{comp}}\rangle \rightarrow -\alpha|\Psi_{\text{in}}^{\text{comp}}\rangle$  for  $\langle 010101|\Psi_{\text{in}}^{\text{comp}}\rangle = 0$ . We first check that a minimum of four ancillas are needed for perfect fidelity. Thus  $N = N_c + N_a = 6 + 4 = 10$ . To reduce the size of the parameter space, and improve the convergence of the success optimization, we consider the following ansatz for  $U$ :  $U_{ij} = U_{ji} = \delta_{ij}$  for  $i = 2, 4, 6$ , i.e.,  $U$  is designed to act non-trivially only on the computational modes 1, 3, and 5. Note that a reduction of “active” modes was also used for the CS gate [2], in full analogy with the one-mode NS gate. However, we find that the construction of Ref. [2] does not work for the Toffoli gate, giving two orders of magnitude smaller success probability (in the CS case both constructions are algebraically equivalent). The results of an optimization over  $10 \times 10$  subunitary matrices are shown in Fig. 3. The best solution obtained is 0.00340; the associated matrix  $U$  has four sub-unitary singular values, corresponding physically to four auxiliary vacuum modes. This is an improvement over combining a CNOT gate, a CS gate, and a “passive quantum filter” to produce the Toffoli gate [3], which yields a total success rate  $S = (2/27)^2 \times 1/2 \approx 0.00274$  using unentangled ancilla resources. We also note that the optimal solution does not make use of the maximal possible number of auxiliary vacuum modes ( $N - 1 = 9$ ); mathematically this is reflected in the fact that the optimal  $10 \times 10$  ma-

trix has a six-fold degeneracy in its largest singular value. As discussed above in connection with the CS gate, this initially surprising result is due to the non-analytic structure of the denominator in Eq. (7), which tends to push the solution toward a degeneracy in the largest singular value.

Interestingly, from a practical point of view, we find that optimization in the full  $10 \times 10$  matrix space produces much more rapid convergence than optimization in  $14 \times 14$  *unitary* space, even though the optimal  $N_v = 4$  solution is an element of both spaces. Paradoxically, optimization in a larger space may yield better convergence! This may be interpreted as follows: in addition to the global maximum, the space of unitary  $U$  contains many local maxima of the success rate, preventing the global maximum from being reached. Eliminating the unitarity constraint creates passageways connecting the local maxima to the global maximum.

In this work, we have provided numerical evidence that the previously obtained solution for the CS (CNOT) gate, with a success probability  $S = 2/27$ , is optimal, and cannot be improved by adding ancillas or auxiliary vacuum modes. On the other hand, for the Toffoli gate we show a new solution, which surpasses what has been obtained analytically using unentangled ancillas. This result is a proof of principle of successful numerical optimization in linear optical quantum information processing. Future directions that naturally suggest themselves include: optimal implementation of two-mode biphotonic qutrit [16] gates; operations on multi-rail encoded qudits using angular momentum photons [20], design of gates that are robust to noise and photon loss, optimization in the context of error-correcting codes [4, 5], and further use of algebraic tools, such as the Gröbner basis [9].

We are grateful to Mark M. Wilde and Pavel Lougovski for very helpful discussions. This work was supported in part by the NSF under Grants No. PHY-0545390 and CRC 0628092, by the Army Research Office, and the Intelligence Advanced Research Projects Activity.

- 
- [1] E. Knill, Phys. Rev. A **68**, 064303 (2003).
  - [2] E. Knill, Phys. Rev. A **66**, 052306 (2002).
  - [3] T. C. Ralph, K. J. Resch, and A. Gilchrist, Phys. Rev. A **75**, 022313 (2007).
  - [4] M. M. Wilde and D. B. Uskov, arXiv:0807.4906v1.
  - [5] S. D. Huver, C. F. Wildfeuer, and J. P. Dowling, arXiv:0805.0296v1.
  - [6] G. D. Durkin, and J. P. Dowling, Phys. Rev. Lett. **99**, 070801 (2007).
  - [7] E. Knill, R. Laflamme, and G. J. Milburn, Nature **409**, 46 (2001).
  - [8] J. Eisert, Phys. Rev. Lett. **95**, 040502 (2005).
  - [9] N. M. VanMeter, P. Lougovski, D. B. Uskov, K. Kieling, J. Eisert, and J. P. Dowling, Phys. Rev. A **76**, 063808 (2007).
  - [10] M. Reck, A. Zeilinger, H. J. Bernstein, and P. Bertani, Phys. Rev. Lett. **73**, 58 (1994).
  - [11] P. Kok, W. J. Munro, K. Nemoto, T. C. Ralph, J. P. Dowling, and G. J. Milburn, Rev. Mod. Phys. **79**, 135 (2007).
  - [12] P. G. Kwiat, Nature **453**, 294 (2008).
  - [13] T. A. Brun, I. Devetak, and M. H. Hsieh, Science **314**, 436 (2006).
  - [14] A. Perelomov, *Generalized Coherent States and Their Applications* (Springer, Berlin, 1986).
  - [15] K. Kraus, *States, Effects and Operations: Fundamental Notions of Quantum Theory* (Springer, New York, 1983).
  - [16] B. P. Lanyon, T. J. Weinhold, N. K. Langford, J. L. O'Brien, K. J. Resch, A. Gilchrist, and A. G. White, Phys. Rev. Lett. **100**, 060504 (2008).
  - [17] M. A. Nielsen and I. L. Chuang, *Quantum Computation and Quantum Information* (Cambridge University Press, 2000).
  - [18] G. G. Lapaire, P. Kok, J. P. Dowling, and J. E. Sipe, Phys. Rev. A **68**, 042314 (2003).
  - [19] I. Bengtsson and K. Życzkowski, *Geometry of Quantum States: An Introduction To Quantum Entanglement* (Cambridge University Press, 2006).
  - [20] J. T. Barreiro, T.-C. Wei, and P. G. Kwiat, Nature **4**, 282 (2008).